Materials Physics and Mechanics. 2022;48(2): 184-198
Research article
http://dx.doi.org/10.18149/MPM.4822022_4

Received: October 7, 2021
Accepted: April 27, 2022

ANALYSIS OF CuCrZr/316L(N) BIMETALLIC JOINT WITH AND WITHOUT NICKEL INTERLAYER FOR PLASMA-FACING COMPONENTS

P. Piskarev[1,2]✉, A. Gervash[1], S. Bobrov[1], V. Ruzanov[1], A. Ogurski[1], I. Mazul[1], R. Giniyatulin[1], B. Ermakov[2], O. Sevryukov[3]

[1]JSC "NIIEFA", St Petersburg, 196641 Russia

[2]Peter the Great St. Petersburg Polytechnic University, St. Petersburg, 195251, Russia

[3]National Research Nuclear University MEPHI, Moscow, 115409, Russia

✉ piskarev@sintez.niiefa.spb.su

Abstract. The work considers the CuCrZr/316L(N) bimetallic joint, which is obtained by diffusion bonding using hot isostatic pressing (HIP) and is a design element of the plasma-facing components (PFC) of a thermonuclear reactor. A comparative analysis of the specified bimetallic joint with a nickel interlayer obtained by different methods and without it has been carried out. A study of the structure and elemental composition of the bimetallic joint was made, where the brittle zirconium phases were identified in the interface zone for all the considered variants. The results of microhardness testing are obtained, demonstrating the presence of a sharp transition of hardness values by more than two times at the interface of two metals. A series of rupture tests of the bimetallic samples was carried out and almost identical values of the rupture stress were obtained for all the considered bimetallic joint variants. The fracture of the samples during the testing at temperatures up to 150°C occurred on the base metal and at higher temperatures – on the bimetallic joint.
Keywords*:* Bimetallic joint, CuCrZr/316L(N), diffusion bonding, Nickel interlayer, brittle layer, plasma-facing components, microhardness, rupture test, embrittlement

Acknowledgements. *The research is partially funded by the Ministry of Science and Higher Education of the Russian Federation as part of World-class Research Center program: Advanced Digital Technologies (contract No. 075-15-2020-934 dated from 17.11.2020)*.

Citation: Piskarev P, Gervash A, Bobrov S, Ruzanov V, Ogurski A et al. Analysis of CuCrZr/316L(N) bimetallic joint with and without Nickel inter-layer for plasma-facing components. *Materials Physics and Mechanics.* 2022;48(2): 184-198. DOI: 10.18149/MPM.4822022_4.

1. Introduction

The low-alloy copper dispersion-hardening alloys, such as CuCrZr, have a number of advantageous characteristics: tensile strength up to 500 MPa at room temperature; maximum operating temperature up to 300°C; values of the thermal and electrical conductivity coefficients at the level of 75-90% of pure copper; corrosion resistance. These characteristics have determined the scope of application of such alloys: products and components operating under the high thermal/electrical and mechanical loads and having active cooling, which allows for maintaining a relatively low operating temperature. One of such applications is the PFC of the thermonuclear reactor [1], which are multilayer structures made of dissimilar metals, including CuCrZr. The density of the heat flux from the plasma on the surface of the PFC reaches 20 MW/m^2. At the same time, the distributed mechanical loads on the PFC from electromagnetic forces are the consequence of the magnetic trap holding the plasma, reaching about 180 kN/m. The CuCrZr alloy in the composition of the PFC acts as a heat-sink layer, which is cooled by water and bonded using brazing with a shielding layer (beryllium/tungsten) on the one hand [2] and by diffusion bonding or explosion bonding with a structural layer (AISI 316L(N)) on the other hand [3,4,5]. For a certain PFC design, the CuCrZr/316L(N) bimetallic joint is located at the water/vacuum boundary (Fig. 1), which leads to strict requirements for the leak tightness of the joint: no more than 1×10^{-11} $Pa\times m^3/s$ at room temperature.

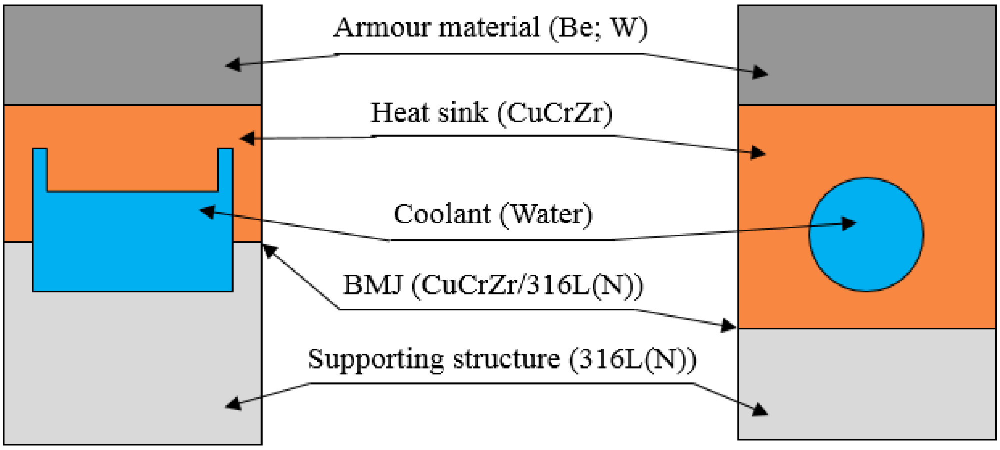

Fig. 1. The cross-section of the various variants of the plasma-facing components with the CuCrZr/316L(N) bimetallic joint

Loss of the bimetallic joint leak tightness under the influence of the operational loads will lead to a loss of the vacuum of the reactor plant and the need for challenging maintenance. The information about such cases is unknown since the PFC of this design has never been used in thermonuclear reactor installations before. However, now there are known cases of destruction considered by the bimetallic joint under the influence of the thermal stresses during the manufacture of the PFC [6,7]. The destruction of the bimetallic joint with a loss of leak-tightness occurred due to the propagation of a crack in the CuCrZr layer along the interface zone.

The well-known feature of the CuCrZr/316L(N) bimetallic joint is a layer with the zirconium phases, which appear in a copper alloy along an interface zone [6-8]. At the same time, the crack noted earlier spreads during the destruction of the bimetallic joint precisely along with the specified layer with zirconium phases [6,7]. The literature notes a method for optimizing the CuCrZr/316L(N) bimetallic joint by introducing an intermediate layer of nickel into the joint [10-12]. The purpose of this work is to study the effect of the nickel interlayer on the chemical composition and characteristics of the CuCrZr/316L(N) bimetallic joint.

2. Materials and Methods

In this work, the study of the CuCrZr/316L(N) bimetallic joint samples with and without a nickel interlayer, made by the diffusion bonding using HIP, was carried out. Four variants of the nickel interlayer were used, differing in the thickness and in the method of the production. Thus, the following types of the CuCrZr/316L(N) bimetallic joint were studied:

1. Without an intermediate layer.
2. With an intermediate layer of nickel foil with a thickness of 25 μm.
3. With an intermediate layer of nickel foil with a thickness of 50 μm.
4. With an intermediate layer in the form of the nickel coating with a thickness of 15 μm on a billet made of CuCrZr.
5. With an intermediate layer in the form of the nickel cover with a thickness of 15 μm on both CuCrZr and 316L(N) blanks.

The chemical composition and the type of the used materials are presented in Table 1.

In order to obtain the bimetallic blanks, the initial blanks of materials after the chemical etching were placed in a capsule, where a vacuum of no worse than 10^{-3} kPa was created. The capsules are processed in a Quintus QIH gas-static press 0.31×0.890-1500-1250 M in the following modes: 150 MPa, 980°C, exposure time 2 hours. Next, the finished bimetallic blanks were "extracted" from the capsule, and the quality of the bimetallic joint was tested by ultrasound control.

The metallographic studies were carried out on the grinds etched in solution (13% $K_2Cr_2O_7$+17% H_2So_4) using the Olympus GX-51 optical microscope with a SIAMS 800 image analysis system and a JEOL JSM-6510LV scanning electron microscope with an E2v X-ray spectral analysis prefix. Microhardness measurements were carried out on the EMCO-TEST DuraScan 50 microhardness meter.

Bimetallic samples were made for the rupture test, which allows conducting the testing according to a special loading scheme. Previously, the bimetallic fabricated parts were heat-treated (HT) in order to obtain optimal CuCrZr mechanical properties [13]: solution annealing (SA) at 980°C for 30 minutes, followed by water quenching, and then aging (A) at 480°C for 2 hours, followed by air cooling. The rupture tests of the bimetallic samples were performed on a universal testing machine Instron 8802 with an Instron SFL 3119-408 climate chamber. The samples assembled with the equipment were heated in the atmosphere. The maximum temperature on the existing equipment is 600°C. The heating time to the maximum temperature was about 2 hours.

3. Research results

Figure 2 shows the micrographs of the sections of the several bimetallic joint variants at magnifications of 100 and 1000 times. The other variants of the bimetallic joint with a nickel interlayer differ visually only in the thickness of the intermediate layer. The average grain size of CuCrZr in all analyzed bimetallic samples is 20-30 μm, and the maximum grain size does not exceed 170 μm.

The CuCrZr/316L(N) bimetallic joint (without an interlayer (Fig. 2, a-b) contains a typical line of phases with a size of 1-2 μm located on the CuCrZr side along with the interface. The CuCrZr/316L (N) bimetallic samples with a nickel interlayer in the form of a foil (Fig. 2, c-d) have a more evident visual interface between the base metals and the intermediate layer, in comparison with the bimetallic joint, which is having a layer in the form of an electrochemical coating (Fig. 2, e-f). This is due to the fact that the electrochemical coating initially has a metallurgical contact with one of the base metals, and the diffusion processes move faster in this case. All the variants of the CuCrZr/316L(N) bimetallic joint with a nickel interlayer do not contain an evident continuous phase line, as in the case of the bimetallic joint without an interlayer but contain separate phases and larger phase lines. These phases are located at the interface of the nickel interlayer and CuCrZr.

An additional study of the CuCrZr/316L(N) bimetallic samples with and without a nickel interlayer after the performed HT (SA + A) showed that there are no changes in the size and density of the phases located in the bimetallic joint zone, and there is no increase in the size of CuCrZr grains.

Table 1. The chemical composition and the type of the used materials

<table>
<tr><th>Material</th><th>The type of the fabricated parts/the method of obtaining</th><th colspan="19">The base elements of the alloy and impurities (wt.%)</th></tr>
<tr><td rowspan="2">CuCrZr</td><td rowspan="2">Hot-rolled sheets</td><td colspan="2">Cu</td><td colspan="2">Cr</td><td colspan="2">Zr</td><td colspan="3">O</td><td colspan="3">Other elements</td><td colspan="7">Other elements in all</td></tr>
<tr><td colspan="2">gen.</td><td colspan="2">0.6 – 0.9</td><td colspan="2">0.07-0.15</td><td colspan="3">Max. Min.</td><td colspan="3">Co <0.05</td><td colspan="7"><0.1</td></tr>
<tr><td rowspan="2">316L(N)</td><td rowspan="2">Cold-rolled sheets</td><td>Fe</td><td>C</td><td>Mn</td><td>Si</td><td>P</td><td>S</td><td>Cr</td><td>Ni</td><td>Mo</td><td>N</td><td>Cu</td><td>B</td><td>Co</td><td>Nb</td><td>Ta</td><td colspan="4">Ti</td></tr>
<tr><td>Gen.</td><td>0.030</td><td>1.60-2.00</td><td>0.50</td><td>0.025</td><td>0.010</td><td>17.00 – 18.00</td><td>12.00– 12.50</td><td>2.30 – 2.70</td><td>0.060 – 0.080</td><td>0.30</td><td>0.0020</td><td>0.05</td><td>0.01</td><td>0.01</td><td colspan="4">0.10</td></tr>
<tr><td rowspan="6">Ni interlayer</td><td rowspan="2">Cold-rolled foil with a thickness of 25 µm</td><td>Ni</td><td>Fe</td><td>C</td><td>Si</td><td>Mn</td><td>S</td><td>P</td><td>Cu</td><td>As</td><td>Pb</td><td>Mg</td><td>Zn</td><td>Sb</td><td>Bi</td><td>Sn</td><td>Cd</td><td colspan="3">Impurities in all</td></tr>
<tr><td>min 99.5</td><td>till 0.1</td><td>till 0.1</td><td>till 0.15</td><td>till 0.05</td><td>till 0.005</td><td>till 0.002</td><td>till 0.1</td><td>till 0.002</td><td>till 0.002</td><td>till 0.1</td><td>till 0.007</td><td>till 0.002</td><td>till 0.002</td><td>till 0.002</td><td>till 0.002</td><td colspan="3"><0.5</td></tr>
<tr><td rowspan="2">Cold-rolled foil with a thickness of 30 µm</td><td>Ni</td><td>Fe</td><td>C</td><td>Si</td><td>Mn</td><td>S</td><td>P</td><td>Co</td><td>Al</td><td>Cu</td><td>As</td><td>Pb</td><td>Mg</td><td>Zn</td><td>O</td><td>Sb</td><td>Bi</td><td>Sn</td><td>Cd</td></tr>
<tr><td>min 99.9</td><td>till 0.03</td><td>till 0.03</td><td>till 0.01</td><td>till 0.002</td><td>till 0.001</td><td>till 0.001</td><td>till 0.1</td><td>till 0.01</td><td>till 0.015</td><td>till 0.001</td><td>till 0.001</td><td>till 0.01</td><td>till 0.002</td><td>till 0.003</td><td>till 0.001</td><td>till 0.001</td><td>till 0.001</td><td>till 0.001</td></tr>
<tr><td rowspan="2">Galvanic cover with a thickness of 15/215 µm</td><td colspan="3">Ni</td><td colspan="16">Impurities</td></tr>
<tr><td colspan="3">100 (Teor.)</td><td colspan="16">The control is not regulated</td></tr>
</table>

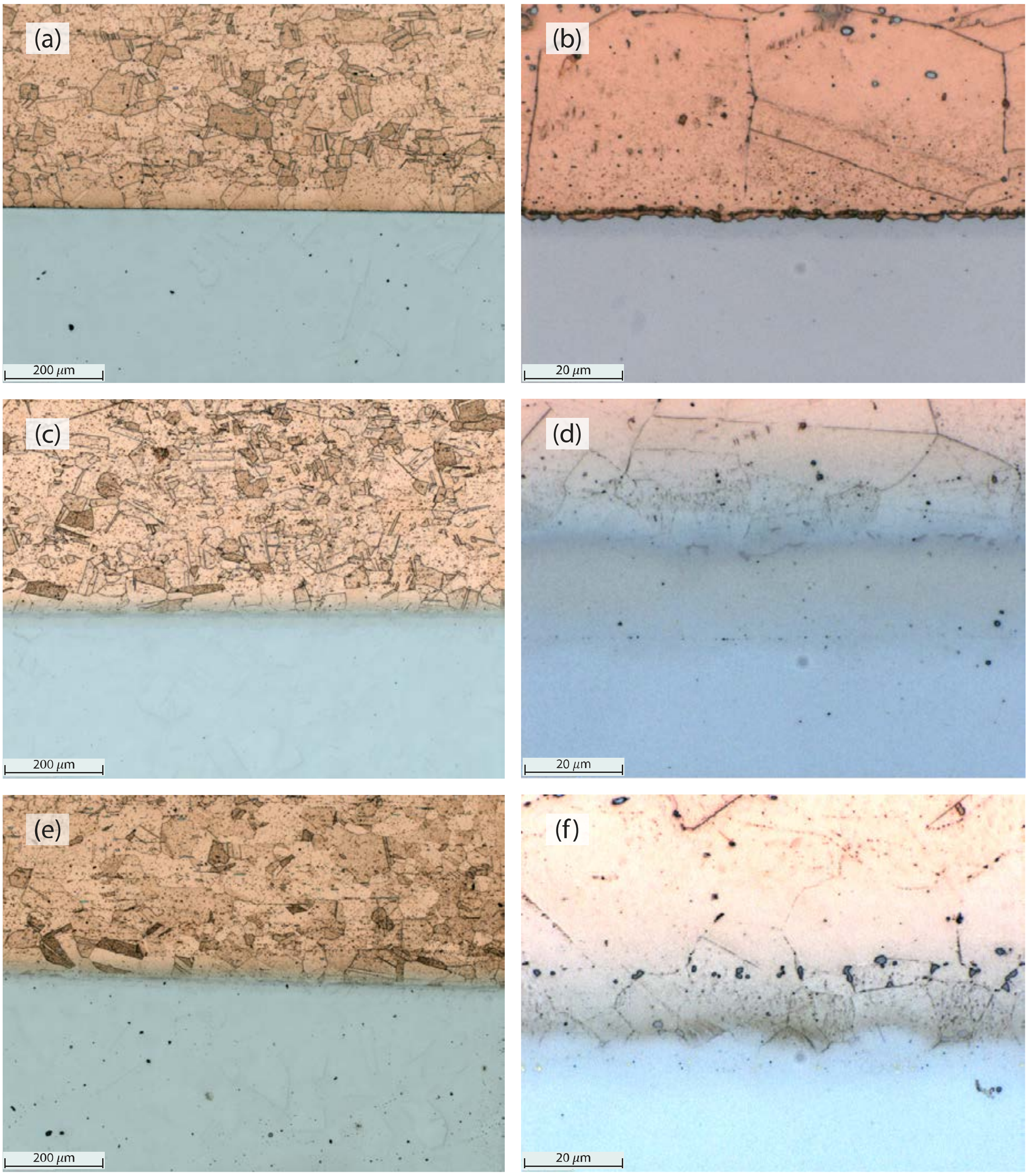

Fig. 2. The micrographs of the CuCrZr/316L(N) bimetallic joint:
(a) Without an intermediate layer (magnification 100 times); (b) Without an intermediate layer (magnification 1000 times); (c) With an intermediate layer in the form of a nickel foil, 25 µm (magnification 100 times); (d) With an intermediate layer in the form of a nickel foil, 25 µm (magnification 1000 times); (e) With an intermediate layer in the form of a nickel coating on both materials, 15 µm (magnification 100 times); (f) With an intermediate layer in the form of a nickel coating on both materials, 15 µm (magnification of 1000 times)

Figure 3 shows the results of the microhardness testing of the CuCrZr/316L(N) bimetallic joint for the several analyzed variants. The results for both variants of the bimetallic joint with a nickel layer in the form of a coating turned out to be almost equivalent, so they are summarized further. The measurements were carried out in sections with a step between shots of about 50 µm.

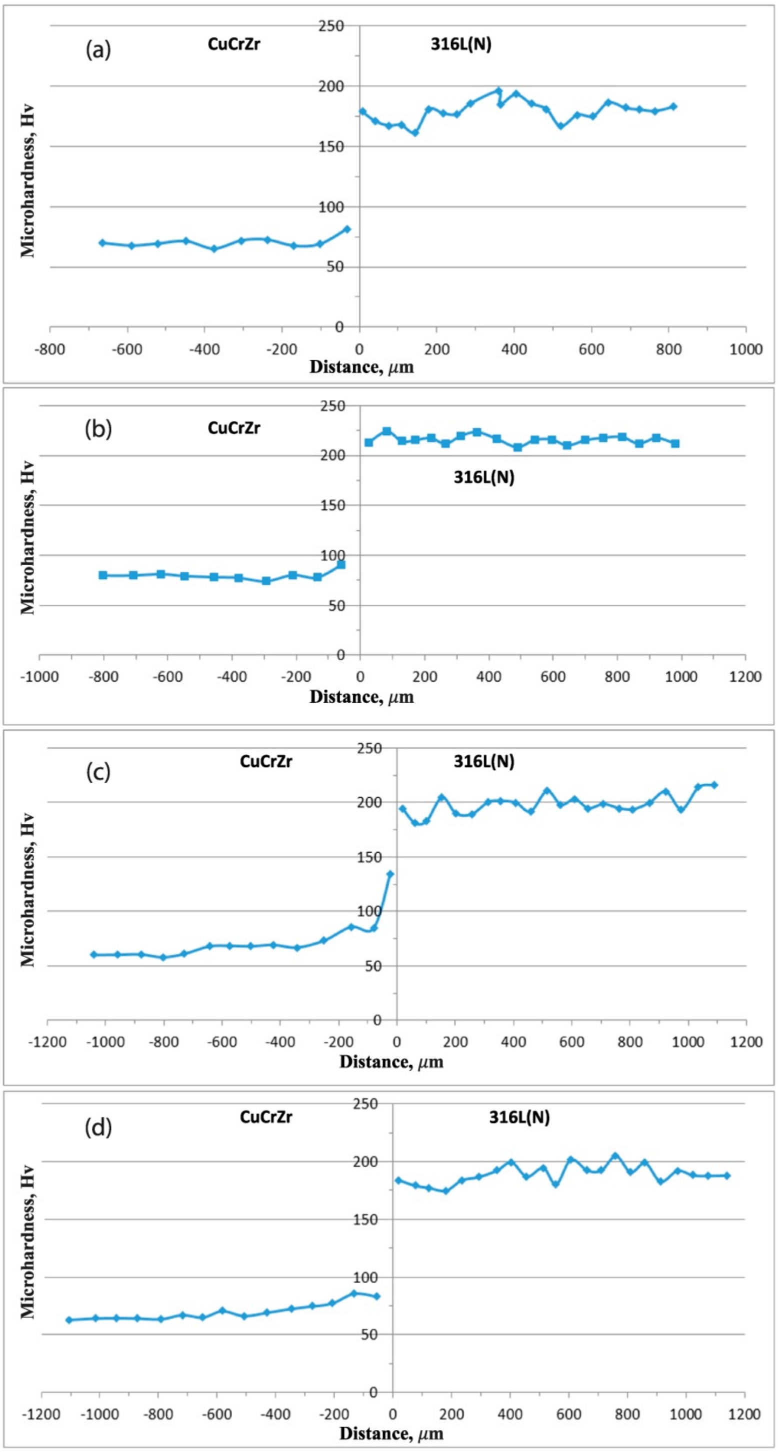

Fig. 3. The results of the microhardness testing of the CuCrZr/316L(N) bimetallic joint: (a) Without an intermediate layer; (b) With an intermediate layer in the form of a nickel foil, 25 µm; (c) With an intermediate layer in the form of a nickel foil, 50 µm; (d) With an intermediate layer in the form of a nickel coating of 15-30 µm.

The hardness of the CuCrZr and 316L(N) differs by more than two times and changes almost abruptly at the interface: on the average, 70 HV for CuCrZr; on average, 180...200 HV for 316L(N). The hardness of CuCrZr after HT (SA + A) is on average 105 HV, the hardness of 316L(N) after is slightly reduced to 160-180 HV. At the same time, the hardness of 316L(N) in the bimetallic joint with a nickel interlayer is on average greater than the hardness of 316L(N) in the bimetallic joint without an interlayer. This fact is probably related to the diffusion of nickel into steel, but this issue requires a separate study. In the current work, the properties of 316L (N) are not analyzed detailed and more attention is paid to CuCrZr, as a weaker metal in the CuCrZr/316L(N) bimetallic joint. The hardness of the nickel interlayer, which was measured for the bimetallic joint with a nickel foil of 50 microns (Fig. 3, c) is about 135 HV. Figure 4 shows a photo of the bimetallic sample with a nickel foil of 50 μm after microhardness testing.

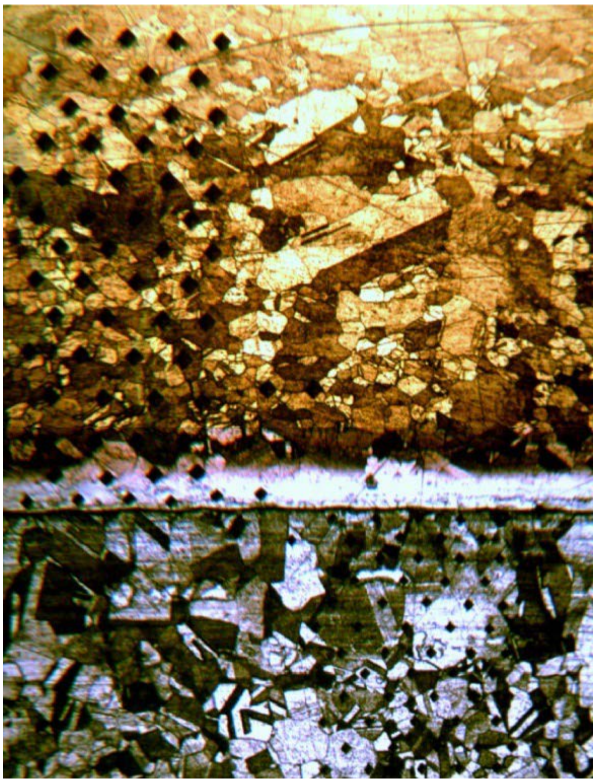

Fig. 4. The photo of the CuCrZr/316L(N) bimetallic sample with an intermediate layer in the form of a nickel foil of 50 μm after microhardness testing

In the structure of the base metal of the analyzed samples, no local increase in hardness was detected since the presence of the large hardening phases or a structure deformed due to mechanical hardening was not detected. In turn, it is impossible to carry out the measurements in the zone of the location of the zirconium phase line using a microhardness tester, due to the small size of the phases and their location near the interface of two metals with different hardness.

Figure 5 shows the results of the X-ray spectral analysis (XRSA) of the CuCrZr/316L(N) bimetallic joint along the line across the interface.

For the CuCrZr/316L(N) bimetallic joint without a nickel interlayer (Fig. 5, a), a peak of zirconium concentration is observed on the CuCrZr side near the interface. On the side of 316L(N), there is a slight increase in the concentration of chromium with a decrease in the concentration of nickel. In the work [7], the structural and phase composition of the boundary layer of 316L(N) in the CuCrZr/316L(N) bimetallic joint was analyzed and the presence of δ-ferrite and σ-phase was revealed. In the current work, the boundary layer of 316L(N) was not analyzed and more attention is paid to the CuCrZr layer, as the weakest material in the bimetallic joint. For all the variants of the CuCrZr/316L(N) bimetallic joint with a nickel interlayer, a similar peak of the zirconium concentration on the CuCrZr side is observed.

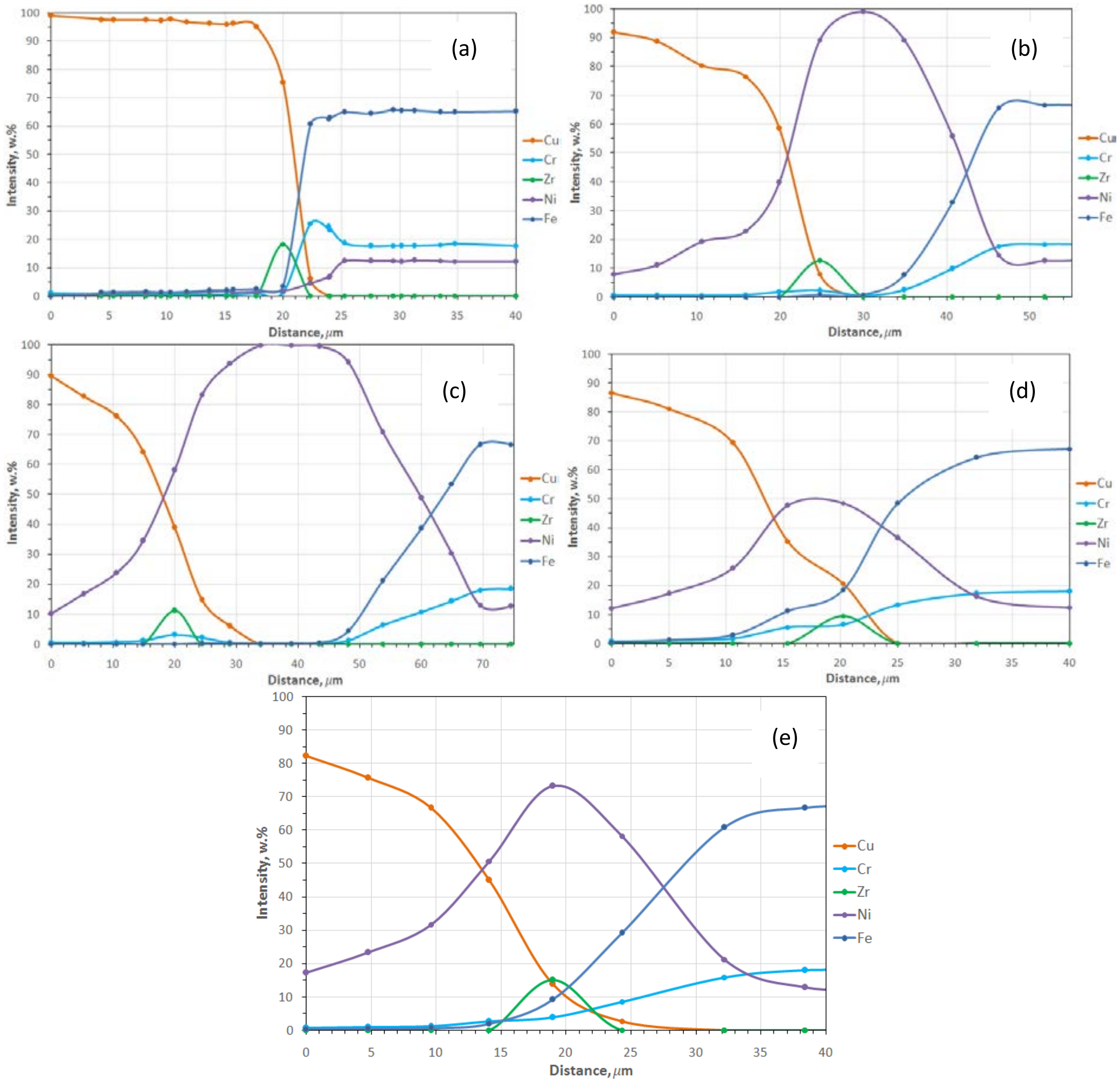

Fig. 5. The results of the XRSA of the CuCrZr/316L(N) bimetallic joint: (a) Without an intermediate layer; (b) With an intermediate layer of nickel foil of 25 μm; (c) With an intermediate layer of nickel foil of 50 μm; (d) With an intermediate layer in the form of a nickel coating on CuCrZr of 15 μm; (e) With an intermediate layer in the form of a nickel coating on CuCrZr and 316L(N), 2×15 μm

Special attention is paid to the analysis of the chemical composition of the zirconium phases in the bimetallic joint without an interlayer because in the literature there are different hypotheses about their chemical composition: intermetallides, carbides, or nitrides of zirconium [7-9]. The results of the XRSA of the CuCrZr layer with zirconium phases are shown in Fig. 6. There are intersecting peaks of the concentration of zirconium and nitrogen, which gives an opportunity to suggest the chemical composition of the phases as zirconium nitride.

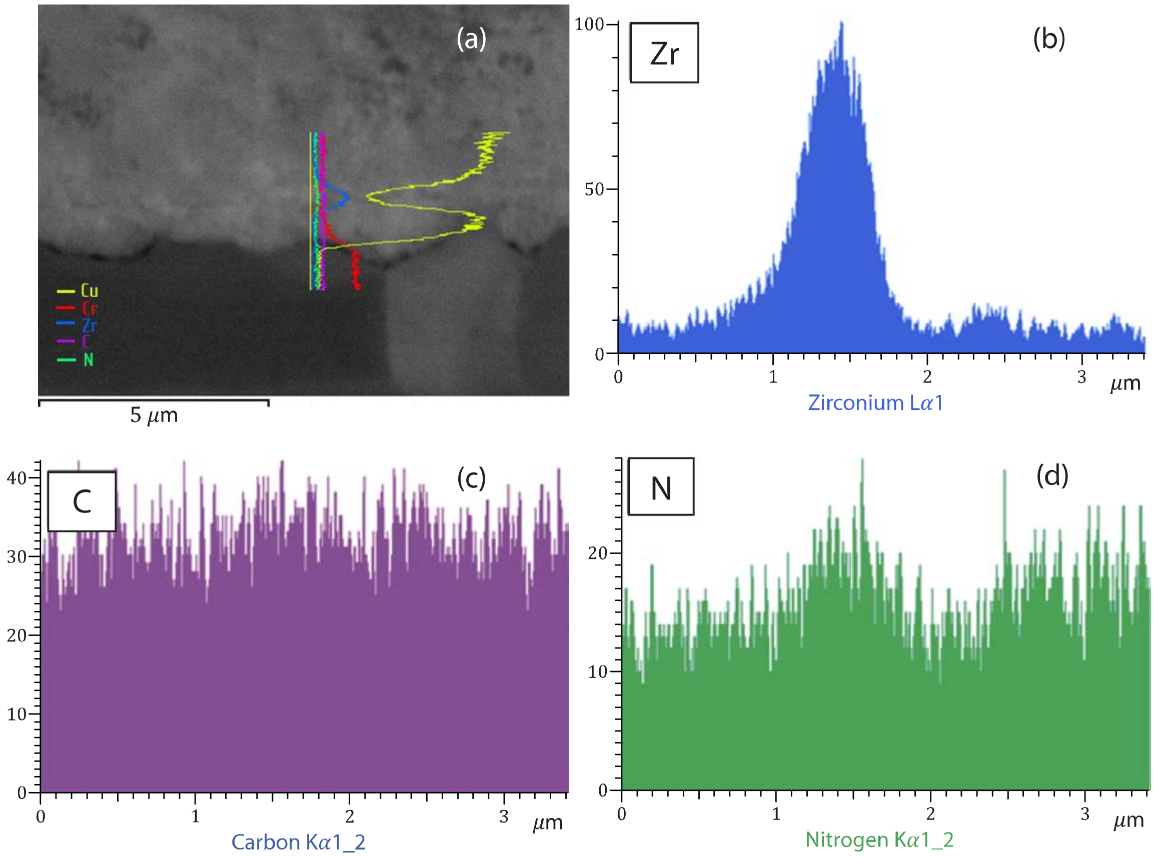

Fig. 6. The results of the XRSA of the zirconium phase layer in the CuCrZr/316L(N) bimetallic joint without an interlayer: (a) the concentrations of the main elements; (b) the concentration of Zr; (c) the concentration of C; (d) the concentration of N

Table 2. The results of the analysis of the zirconium phases

<table>
<tr><th colspan="2">CuCrZr/316L (N)</th><th>Spectrum №</th><th colspan="6">The elemental composition of the spectrum</th><th>The chemical composition of the phase</th></tr>
<tr><td colspan="2" rowspan="2">Without interlayer (Fig. 7, a)</td><td rowspan="2">1</td><td>Zr, weight. %</td><td>N, weight. %</td><td>result, weight. %</td><td>Zr, at.%</td><td>N, at.%</td><td>result, at.%</td><td rowspan="2">ZrN</td></tr>
<tr><td>89,55</td><td>10,45</td><td>100,00</td><td>56,82</td><td>43,18</td><td>100,00</td></tr>
<tr><td rowspan="6">With a nickel interlayer in the form of</td><td rowspan="4">foil (Fig. 7, b)</td><td>-</td><td>Zr, weight. %</td><td>Ni, weight. %</td><td>result, weight. %</td><td>Zr, at.%</td><td>Ni, at.%</td><td>result, at.%</td><td>-</td></tr>
<tr><td>1</td><td>27.73</td><td>72.27</td><td>100.00</td><td>19.81</td><td>80.19</td><td>100.00</td><td rowspan="3">Ni_5Zr</td></tr>
<tr><td>2</td><td>27.68</td><td>72.32</td><td>100.00</td><td>19.76</td><td>80.24</td><td>100.00</td></tr>
<tr><td>3</td><td>26.44</td><td>73.56</td><td>100.00</td><td>18.79</td><td>81.21</td><td>100.00</td></tr>
<tr><td rowspan="2">cover (Fig. 7, c)</td><td>1</td><td>31.18</td><td>68.82</td><td>100.00</td><td>22.58</td><td>77.42</td><td>100.00</td><td rowspan="2">Ni_7Zr_2</td></tr>
<tr><td>2</td><td>31.67</td><td>68.33</td><td>100.00</td><td>22.98</td><td>77.02</td><td>100.00</td></tr>
</table>

The micro-XRSA of the individual zirconium phases allowed us to clarify the assumptions about their chemical composition for all analyzed variants of the bimetallic joint. Figure 7 shows the electronic images of the studied phases, and Table 2 shows their elemental composition. The results for both variants with a nickel foil, as well as both variants with a nickel coating, were identical, so they are summarized further. According to Ni-Zr diagram, the chemical composition of the phases of the zirconium nickelides is identified. Table 2 presents the results of the micro-XRSA for all bimetallic joint variants.

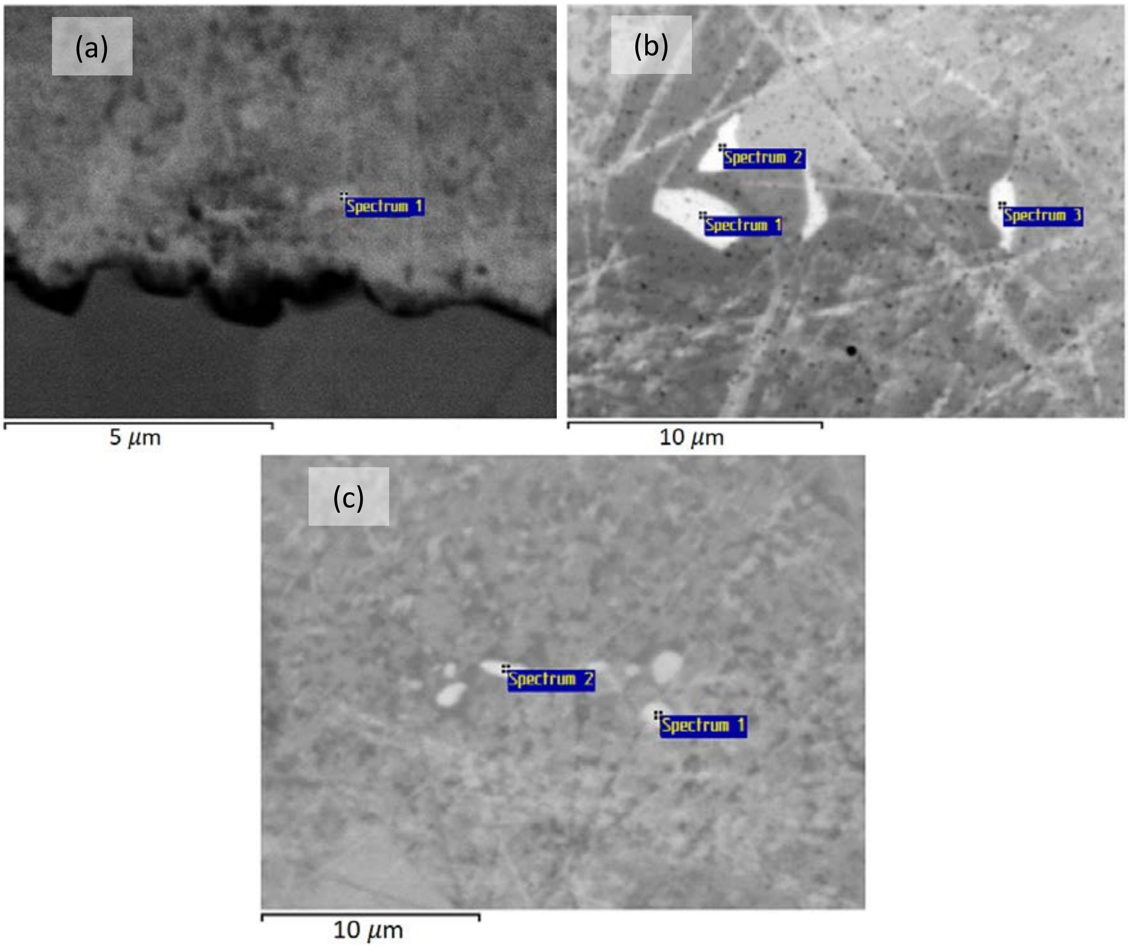

Fig. 7. The analysis of the chemical composition of the zirconium phases:
(a) the bimetallic joint without an interlayer; (b) the bimetallic joint with a foil interlayer;
(c) the bimetallic joint with an interlayer in the form of a coating

In the case, where the nickel foil is used as an interlayer, Ni_5Zr intermetallic phases are formed in the bimetallic joint zone. In the case of a nickel coating, Ni_7Zr_2 phases are formed and the location density of phases in the bimetallic zone is higher, which indicates a greater amount of zirconium involved in the formation of this layer. Nickel is initially applied to the surface of CuCrZr in the form of a coating, which leads to a faster interaction with zirconium during the HIP.

The rupture tests of the bimetallic samples were performed at three temperature levels. The test results are presented in Table 3.

Table 3. Test results of bimetallic samples

The type of the bimetallic joint CuCrZr/316L(N)		The test results at a given temperature (averaged)					
		RT		150°C		600°C	
		Rupture stress, MPa	Fracture zone	Rupture stress, MPa	Fracture zone	Rupture stress, MPa	Fracture zone
Without interlayer		431	CuCrZr	367	CuCrZr	115	The bimetallic joint
With the nickel interlayer	Foil with a thickness of 25 µm	426	CuCrZr	368	CuCrZr	128	The bimetallic joint
	Foil with a thickness of 50 µm	425	CuCrZr	373	CuCrZr	133	The bimetallic joint
	Foil with a thickness of 15 µm on CuCrZr	426	CuCrZr	369	CuCrZr	112	The bimetallic joint
	Foil with a thickness of 15 µm on CuCrZr and 316L(N)	422	CuCrZr	371	CuCrZr	118	The bimetallic joint

The value of the rupture stress for all the variants of the bimetallic joint at room temperature and 150°C differ by no more than 2%, and at 600°C – up to 20%. At the same time, higher values of the rupture stress at elevated temperatures are observed for the variants with an intermediate layer of nickel foil. However, the increased spread of the values at the maximum temperature is probably a consequence of lower test statistics (2-3 samples of each type). The fracture types of the samples for all the bimetallic joint variants are the same: the fracture of the base metal at the temperature of up to 150°C and the fracture of the joint zone at the maximum temperature. For example, the bimetallic samples without the intermediate layer after testing are shown in Fig. 8. Samples with a nickel interlayer have a similar view.

Fig. 8. The photos of the bimetallic samples after the rupture tests

The results of the XRSA of the fracture surface on the tested samples at the maximum temperature indicate fracture along with the layer with the inclusions of the zirconium phases: a similar spectrum is observed with an evident zirconium peak on both parts of the tested sample. For example, Fig. 9 shows the analyzed spectrum of the fracture surface of the bimetallic samples with and without nickel interlayer.

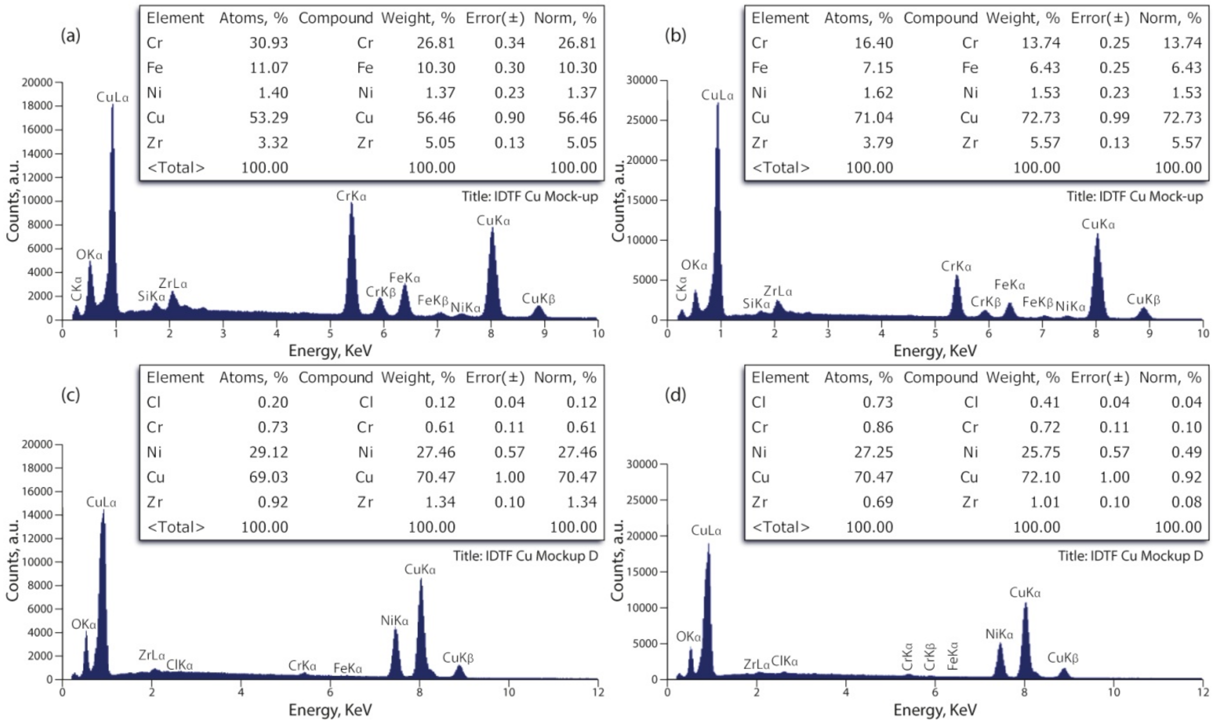

Fig. 9. The XRSA of the fracture surface of the bimetallic samples with and without nickel interlayer: (a) the surface of the CuCrZr part of the sample without nickel interlayer; (b) the surface of the 316L(N) part of the sample without nickel interlayer; (c) the surface of the CuCrZr part of the sample with nickel interlayer; (d) the surface of the 316L(N) part of the sample with nickel interlayer

Probably, the fracture of the bimetallic samples and the cases of the destruction of the bimetallic joint in the PFC (as indicated in the introduction) are the results of the same feature. However, unlike the PFC, where all the HT operations are performed in a vacuum, the heating of the bimetallic samples before testing is performed in the atmosphere. Therefore, it is necessary to exclude the influence of the oxidation of the surface of the samples on the feature of the fracture during the rupture tests. For this purpose, two series of additional rupture tests were performed. In the first case, a corrosion-resistant nickel coating was applied to the surface of the bimetallic samples. The thickness of the coating of 30 μm was selected experimentally for specific heating conditions. These samples were tested at a maximum temperature of 600°C. In the second case, the samples were heated before testing in the atmospheric furnace to a target temperature of 600°C and cooled after 0.5 hours of exposure. Further, the samples were tested at room temperature. Both types of samples after the testing are shown in Fig. 10.

Regardless of the presence of surface oxidation during heating, the fracture of the samples during the rupture tests occurred as before: on the bimetallic joint at maximum temperature; on the base metal at room temperature.

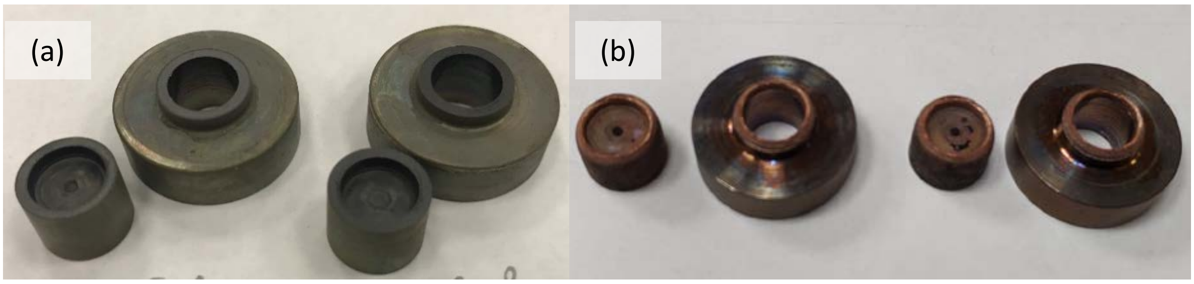

Fig. 10. The photos of the bimetallic samples after the additional tests:
(a) sample with corrosion-resistant nickel coating tested at 600°C; (b) sample pre-heated at 600°C and tested at room temperature

4. Discussion of results

The comparative analysis performed by the metallographic methods demonstrates a clear difference between the considered variants of the CuCrZr/316L(N) bimetallic joint with a nickel interlayer and the variant without an interlayer. Instead of an evident layer of zirconium nitrides in the bimetallic joint without an interlayer, invariants with a nickel interlayer, there are separate phases and short lines of zirconium intermetallides. However, these changes in the structure do not significantly affect the analyzed characteristics of the CuCrZr/316L(N) bimetallic joint.

For all the considered variants of the bimetallic joint, the hardness values change more than twice at the interface between CuCrZr and 316L(N) by a "jump" (sharply). Such an interface between two metals with these differences in properties can itself be a stress concentrator that weakens the bimetallic joint, which may be one of the reasons for the destruction of the joint in samples/components. The layer of the zirconium phases also weakens the bimetallic joint. Moreover, the results of the rupture tests of the bimetallic samples demonstrate a clear dependence of the type of fracture of samples on the temperature conditions of the test. With an increase in the temperature, the type of fracture changes from the viscous fracture in the base metal to fracture in the bimetallic joint. Probably, in this case, the influence of the "ductility failure", which is peculiar to most copper alloys, is observed [14]. In a certain range of elevated temperature, the ductility properties of CuCrZr decrease, which, together with the previously mentioned structural features of the CuCrZr/316L(N) bimetallic joint (an interface with a sharp transition of hardness; a layer with zirconium phases), leads to an increase in the stress level in the bimetallic joint of the components/sample and subsequent destruction along the joint. Taking into account all the above, it is impossible to single out and evaluate separately the level of influence of each structural feature of the CuCrZr/316L(N) bimetallic joint on its characteristics without additional research.

Based on the results of the conducted work, we can suggest, that the intermediate layer of nickel, obtained by each of the considered methods does not lead to the significant changes in these features of the bimetallic joint. Although, the value of the microhardness of the nickel layer, which was tested for 50 μm interlayer of foil, was the intermediate value between CuCrZr and 316L(N). Therefore, the nickel interlayer provides a smoother transition of the hardness values in the CuCrZr/316L(N) bimetallic joint. In other works, a positive influence of the nickel interlayer on such characteristics of bimetallic joint as impact strength is noted [12]. Probably, under the dynamic loads, the nickel interlayer of the bimetallic joint performs the role of a "damping" layer. With reference to the current work, it is planned to conduct additional mechanical tests of the CuCrZr/316L(N) bimetallic samples with and without a nickel interlayer, as well as to perform a more detailed study of the previously listed features of this bimetallic joint.

5 Conclusions

The method of optimizing the CuCrZr/316L(N) bimetallic joint by introducing an intermediate layer of nickel does not lead to a significant change in the characteristics of the bimetallic joint, defined as design criteria for the PFC. The nickel interlayer affects the chemical composition of the bimetallic joint, however, it does not completely exclude the formation of brittle phases of zirconium along with the interface. The conducted tests of the bimetallic samples with and without a nickel interlayer demonstrated almost identical results for the compared variants. At the same time, all the bimetallic samples during the tests at the elevated temperature up to ~600° fracture in the bimetallic joint. Probably, the known cases of the destruction of the bimetallic joint in the PFC and the specified cases of the fracture of the bimetallic samples are associated with the same features of the considered bimetallic joint. Therefore, the urgent task is to conduct further studies of the features of the CuCrZr/316L(N) bimetallic joint and find out the decision for its optimization.

References

[1] Raffray AR, Nygren R, Whyte DG, Abdel-Khalik S, Doerner R, Escourbiac F, Evans T, Goldston RJ, Hoelzer DT, Konishi S, Lorenzetto P, Merola M, Neu R, Norajitra P, Pitts RA, Rieth M, Roedig M, Rognlien T, Suzuki S, Tillack MS, Wong C. High heat flux components—Readiness to proceed from near term fusion systems to power plants. *Fusion Engineering and Design*. 2010;85(1): 93-108.

[2] Gervash AA, Giniyatulin RN, Guryeva TM, Glazunov DA, Kuznetsov VE, Mazul IV, Ogursky AY, Piskarev PY, Safronov VM, Eaton R, Raffray R, Sevryukov ON. The development of technology of Be/CuCrZr joining using induction brazing. *Fusion Engineering and Design*. 2019;146: 2292-2296.

[3] Gervash AA, Glazunov DA, Lyanzberg DV, Mazul IV, Ogursky AY, Piskarev PY, Ruzanov VV. Refinement of the technology of hot isostatic pressing of vacuum-tight bimetallic joint of ITER in-Vessel components. In: *Innovative Designs and Technologies of Nuclear Power: Collection of papers of V International Scientific and Technical Conference*. Moscow: Publishing House of JSC "NIKIET"; 2018. p.2428-2434.

[4] Xu JF, Yang M, Ma HH, et al. Fabrication and performance studies on explosively welded CuCrZr/316L bimetallic plate applied in extreme environments. *Journal of Materials Research and Technology*. 2020;9(4): 8971-8984.

[5] Gonzalez JM, Chiumenti M, Cervera M, Agelet de Saracibar C, Samaniego F, Cobo I. Numerical analysis of the manufacturing processes of a mock-up of the ITER NHF First Wall Panel. *Fusion Engineering and Design*. 2018;135: 65-73.

[6] Piskarev PY, Gervash AA, Ogursky AY, Mazul IV, Ruzanov VV, Bobrov SV, Khokholov MV, Lyanzberg DV. Formation of brittle layers during hot isostatic pressing of bimetal joints of ITER components. In: *46th International Conference on Plasma Physics and CF*. Zvenigorod; 2019. p.259.

[7] Piskarev PY, Gervash AA, Vologzhanina SA, Ermakov BS. Analysis of the Destruction of a diffusion bimetallic compound CuCrZr-IG / 316L(N)-IG obtained under hot isostatic pressing. In: *International symposium 'Nanophysics and Nanomaterials*. St. Petersburg: Saint-Petersburg Mining University; 2020. p.258-264.

[8] Goods SH, Puskar JD. Solid state bonding of CuCrZr to 316L stainless steel for ITER applications. *Fusion Engineering and Design*. 2011;86: 1634-1638.

[9] Ordas N, Samaniego F, Iturriza I, Gomez A, Escudero C, Fernandez-Calvo AI, Cobo I, Banetta S, Heikkinen S, Cicero T. Mechanical and microstructural characterization of HIP joints of a simplified prototype of the ITER NHF First Wall Panel. *Fusion Engineering and Design*. 2017;124: 999-1003.

[10] Marois GLe, Dellis Ch, Gentzbittel JM, Moret F. HIP'ing of copper alloys to stainless steel. *Journal of Nuclear Materials*. 1996;233-237: 927-931.

[11**]** Singh KP, Alpesh Patel, Kedar Bhope, Khirwadkar SS, Mayur Mehta. Optimization of the diffusion bonding parameters for SS316L/CuCrZr with and without Nickel interlayer. *Fusion Engineering and Design.* 2016;112: 274-282.
[12] Wei R, Zhao SX, Dong H, Che HY, Li Q, Wang WJ, Wang JC, Wang XL, Sun ZX, Luo GN. Enhancing the CuCrZr/316L HIP-joint by Ni electroplating. *Fusion Engineering and Design*. 2017;117: 58-62.
[13] Mayo Diaz MA, Gustavo ME. Effect of Solution Treatment in CuCrZr Alloy Structure. *AASCIT Journal of Materials*. 2017;3(3): 14-18.
[14] Laporte V, Mortensen A. Intermediate temperature embrittlement of copper alloys. *International Materials Reviews*. 2009;54(2): 94-116.

THE AUTHORS

Piskarev P.Y.
e-mail: piskarev@sintez.niiefa.spb.su
ORCID: 0000-0002-8551-9594

Gervash A.
e-mail: gervash@sintez.niiefa.spb.su
ORCID: 0000-0002-5376-3787

Bobrov S.
e-mail: bobrov@sintez.niiefa.spb.su
ORCID:

Ruzanov V.
e-mail: ruzanov@sintez.niiefa.spb.su
ORCID: 0000-0002-3343-1769

Ogurski A.
e-mail: ogursky@sintez.niiefa.spb.su
ORCID: 0000-0001-8274-4852

Mazul I.
e-mail: mazul@niiefa.spb.su
ORCID: 0000-0001-9381-1600

Giniyatulin R.
e-mail: radmir.giniiatulin@iter.org
ORCID: 0000-0002-4067-5374

Ermakov B.
e-mail: ermakov_bs@spbstu.ru
ORCID:

Sevryukov O.
e-mail: sevr54@mail.ru
ORCID: 0000-0002-8711-8962